Electro-optic behaviour of a non-polar nematic liquid crystal and its mixtures

N. Scaramuzza[a]; G. Strangi[a]; C. Versace[a]

[a] Dipartimento di Fisica dell'Universita degli Studi della Calabria and Istituto Nazionale per la Fisica della Materia UdR della Calabria, I-87036 Arcavacata di Rende (Cosenza), Italy,

PLEASE SCROLL DOWN FOR ARTICLE

Electro-optic behaviour of a non-polar nematic liquid crystal and its mixtures

N. SCARAMUZZA*, G. STRANGI and C. VERSACE

Dipartimento di Fisica dell'Università degli Studi della Calabria and Istituto
Nazionale per la Fisica della Materia UdR della Calabria,
I-87036 Arcavacata di Rende (Cosenza), Italy

In this work we report preliminary results on the properties of a non-polar bicyclohexane nematic liquid crystal. Moreover, its binary mixtures both with a low viscosity phenylcyclohexane and with a normal polar nematic liquid have been investigated. The elastic, viscous and electro-optical properties of these compounds are presented. The non-polar compound, and its mixture with a low percentage of the well known liquid crystal MBBA, exhibit an electrohydrodynamic behaviour in which the conducting regime is absent, while the dielectric regime spreads to low frequencies. Additionally, at higher frequencies of the applied electric field, a regime whose thresholds are linear in frequency is observed. On the other hand, the mixture formed by 50 wt % of the non-polar compound with MBBA exhibits at low frequencies the usual behaviour, followed at higher frequencies by the linear regime.

1. Introduction

Liquid crystals formed by non-polar molecules are of great interest from both an applicative and a fundamental point of view. The mesophases given by non-polar compounds show several characteristics (high purities, low viscosity and low electrical conductivity) that make them suitable for liquid crystal mixtures for display applications. Moreover, they allow studies of electrostatic and electrodynamical phenomena which are present in dielectrics in general, and in liquid crystals in particular, without the effects resulting from coupling between applied electric fields and molecular dipoles.

The subject of this work is a new mesogen, known in the literature as $0d_3CCO2$ (by Rolic) [1]; it belongs to the non-polar bicyclohexane liquid crystal class that exhibits pronounced nematic mesophases. Mixtures of $0d_3CCO2$ with the low viscosity phenylcyclohexane $3CPOd_31$ (by Rolic) [1] and with the liquid crystal N-(p-methoxybenzilidene)-p-n-butylaniline (MBBA, by the Eastman Kodak Co.), have been also studied.

2. The Fréedericksz transition

In figure 1 (*a*), a nematic liquid with negative dielectric anisotropy (e.g. MBBA, $\Delta\varepsilon = \varepsilon_\parallel - \varepsilon_\perp = -0.7$ [2, 3]) is

*Author for correspondence; e-mail: scaramuzza@fis.unical.it
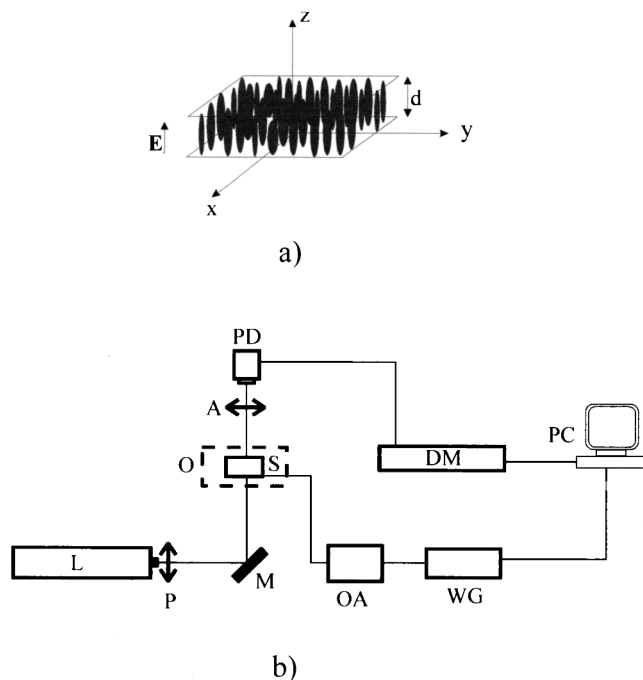

Figure 1. (*a*) Experimental geometry. Homeotropic texture: $d =$ sample thickness; **E** = applied electric field. (*b*) Experimental set-up: L = HeNe laser; P = polarizer; M = mirror; O = oven; S = liquid crystal sample; A = analyser; PD = photodiode; DM = digital multimeter; WG = waveform generator; OA = amplifier; PC = computer.

inserted between two semi-transparent ITO electrodes. The unperturbed molecular director **n** lies perpendicular to the glass plate boundaries and an external electric voltage V is applied across the nematic film. As long as V exceeds a threshold value, V_{th}, this experimental geometry allows us to observe the electrically controlled birefringence (ECB) effect. The voltage V_{th} is given by [3]:

$$V_{th} = \pi(4\pi K_{33}/|\Delta\varepsilon|)^{1/2} \qquad (1)$$

where K_{33} is the Frank elastic constant of bend.

The sample birefringence can be evaluated by recording the voltage behaviour of the light intensity that is transmitted by the NLC cell placed between two crossed polarizers. Let us consider a monochromatic and linearly polarized light beam of wavelength λ that impinges on the glass plates of the cell at normal incidence. The zero-voltage intensity of the light passing through an analyser whose direction is perpendicular to the light polarization is zero, or at least negligible. Increasing V below V_{th}, the NLC director reorients (B-effect), the phase difference $\Delta\phi$ between the extraordinary and ordinary rays of the monochromatic light starts to increase and some light intensity I will cross the analyser. Initially at $V \cong V_{th}$, I increases linearly with $\Delta\phi$. At higher voltage it oscillates according to the formula:

$$\frac{I}{I_0} = \sin^2\frac{\Delta\phi}{2}.$$

The final orientation of the director is not defined; the sample does not remain monodomain and contains many umbilic defects [4].

The maximum possible number of oscillations (i.e. the number N of maxima during a complete reorientation of the director) is approximately [2, 3]:

$$N = (n_\parallel - n_\perp)d/\lambda = \Delta n d/\lambda \qquad (2)$$

where d is the cell thickness, and $n_\parallel$ and $n_\perp$ represent the extraordinary and ordinary refractive indexes, respectively.

Under the same experimental geometry, it is possible to induce a dynamical Fréedericksz transition. The characteristic response times connected with the distortion of the molecular director field, in the small distortion limit,

have been derived in [3]:

$$\tau_{on} = \gamma_1^*/[(\Delta\varepsilon \mathbf{E}^2/4\pi) - (K_{33}\pi^2/d^2)] \qquad (3a)$$

$$\tau_{off} = \gamma_1^*/(K_{33}\pi^2)/d^2 \qquad (3b)$$

where τ_{on} is the switch-on time, and τ_{off} is the switch-off, decay or relaxation time. The effective rotational viscosity γ_1^* (which takes into account the back-flow that considerably alters the response times) for the B-effect, is given by:

$$\gamma_1^* = \gamma_1 - (2\alpha_2^2/\alpha_4 + \alpha_5 - \alpha_2) \qquad (4)$$

where $\gamma_1 = \alpha_3 - \alpha_2$ the rotational viscosity, and α_2, α_3, α_4 and α_5 are the Leslie viscosity coefficients [5].
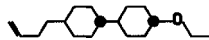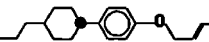
2.1. *Experiments and results*

The table shows the new compounds which exhibit nematic mesophases. The binary mixture M7 is obtained by combining the bicyclohexane component $0d_3$CCO2 (in the following indicated using the acronym NP) with the compound, $3CPOd_3$1 (*E*)-2-butenyloxy-4-(*trans*-4-propylcyclohexyl)benzene [1]. The characterization of these materials has been established by several spectroscopic techniques, as well as by electro-optic techniques, light scattering, and microscopy with polarized light.

The experimental geometry shown in figure 1 allowed us to study both the viscous and elastic properties which govern the statics and the dynamics of the Fréedericksz transition. The experiments were always performed on sandwich-like cells with homeotropic alignment. The homeotropic alignment of the molecules was achieved by a silane coating (DMOAP, by Thomson CSF) applied by dipping the ITO coated glass plates in a 0.1 wt % solution of DMOAP in isopropyl alcohol. Subsequently the glass plates were washed in water and then cured at 110°C for 1 h. The quality of the homeotropically aligned samples was checked by conoscopic observation using a polarizing microscope (Axioskop Pol, by Zeiss).

The first experiment concerns the study of the electrically controlled birefringence (ECB) effect. The experimental set-up is shown in figure 1(*b*). The temperature of the sample was controlled by mean of a brass holder with a Teflon jacket, thermostatted at 25.0 ± 0.1°C by

Table. Single non-polar component $0d_3$CCO2, single component $3CPOd_3$1 and their binary mixture M7. All are nematic and the transition temperatures quoted are from [1].

Nomenclature	Structure	Melting temperature/°C	Nematic–isotropic transition temperature/°C
$0d_3$CCO2		13.1	45.3
$3CPOd_3$1		42.4	57.5
M7 = (od_3CCO2, 3CPO$d_3$1) (50:50 mol %)		< 15	44.5

circulating ethylene glycol from a HAAKE F3 thermostat. The thickness of all the samples was fixed by $100\,\mu m$ thick Mylar spacers. The applied oscillating (1 kHz) voltage was supplied by a bipolar amplifier KEPCO Model B0P 500M driven by a waveform generator 8904A (Hewlett Packard). The intensity of a monochromatic light beam (5 mW HeNe laser) transmitted by the sample between crossed polarizers, was detected by a photodiode. Then the amplified electric signal arising from the photodiode was sent to a digital 3478A multimeter (Hewlett Packard). Both waveform generator and digital multimeter were connected to a PC.

In order to test the experimental apparatus we carried out some measurements on the cell filled with the well known liquid crystal MBBA [2]. Figures 2(a), 2(b) and 2(c) show the voltage behaviour of the light intensity I transmitted by the cells filled with M7, NP and MBBA, respectively.

In case of well homeotropically oriented NLC cells, the B-effect is characterized by a steep growth of the optical transmission I vs. the voltage V, i.e. the threshold is very abrupt. The threshold voltages V_{th} were found to be 5.9 ± 0.1 and 6.2 ± 0.1 V for NP and M7, respectively.

By studying the dynamics of the Fréedericksz transition we derived the characteristic times τ_{on} and τ_{off}. The experiments were performed using the same experimental set-up; the time behaviour of the transmitted light intensity was recorded during the transients which correspond, respectively, to the switching-on and the switching-off of the applied oscillating field. The measured τ_{on} and τ_{off} vs. the applied electric field for both the compound NP and the mixture M7 are shown, respectively, in figures 3(a) and 3(b).

From an experimental point of view it was not possible to obtain direct information on the values of Δn for the materials under investigation. In fact, for safe cell operation we did not apply a very strong voltage ($V_{max} < 40$ V), and so did not obtain complete reorientation of the molecular director.

The quantification of the B-effect of MBBA, compared with that of NP and M7, allows us to obtain a rough
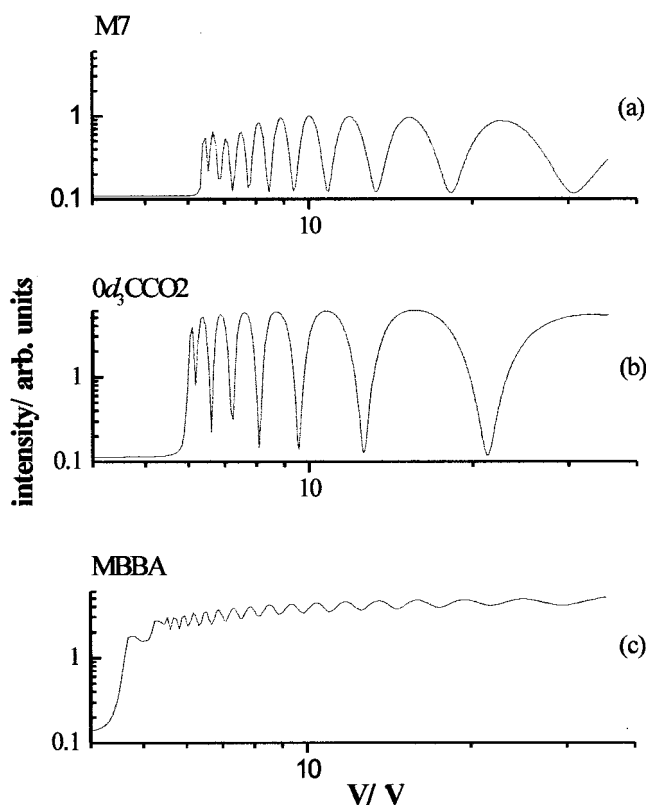

Figure 2. Typical oscillating dependence on voltage of the optical transmission from the cells placed between crossed polarizers. In (a) is shown the response of M7, in (b) of NP, the non-polar compound $0d_3CCO_2$ and in (c) of MBBA.

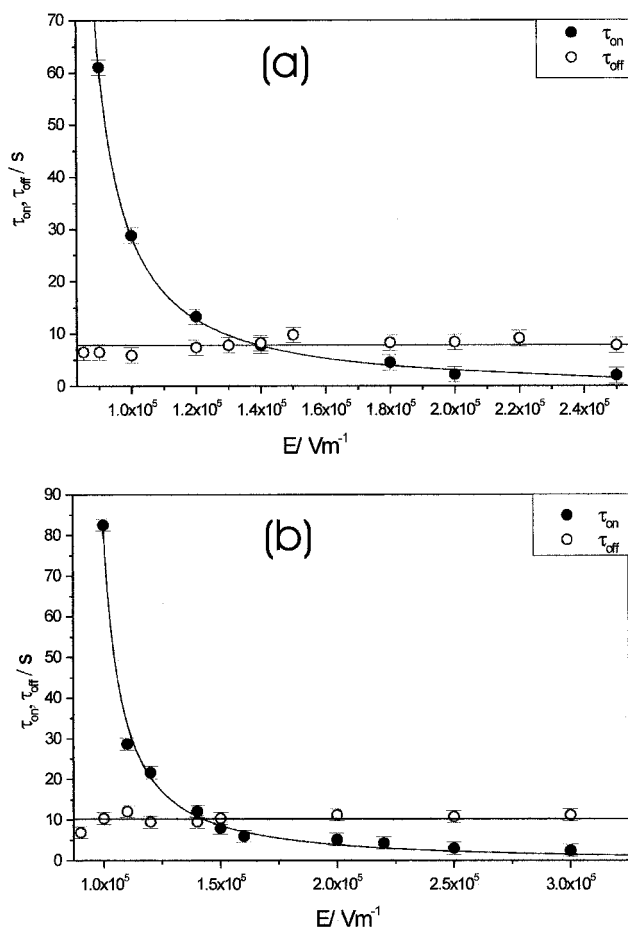Figure 3. The switching times τ_{on} (black circles) and the relaxation times τ_{off} (open circles) versus the applied electric field for (a) $0d_3$CCO2 and (b) its mixture M7. Both samples were homeotropically aligned. The two full straight lines represent the average values of the τ_{off} times. The full lines connecting the τ_{on} times, represent the best fits made by means of equation (3).

value of Δn for both the non-polar compound and the mixture M7. Let us consider the equation (2) written for MBBA and for NP, respectively:

$$N_{\text{MBBA}} = (\Delta n)_{\text{MBBA}} \times 100\,\mu\text{m}/\lambda$$
$$N_{\text{NP}} = (\Delta n)_{\text{NP}} \times 100\,\mu\text{m}/\lambda.$$

Obviously, N must be calculated over the same range of applied voltage for both materials. By calculating the ratio between the two expressions, and using the value of $(\Delta n)_{\text{MBBA}} = 0.21$ [2, 3], we obtained for the material NP a value of $\Delta n \approx 0.08$. By using the same procedure for M7, we obtained a value of $\Delta n \approx 0.11$. For M7, the value of the optical anisotropy reported in [1] (measured by Abbé refractometry using a prism giving homogeneous alignment) is $\Delta n = 0.074$ at 22°C. Up to now, to our knowledge, there are no data in the literature regarding the value of Δn for NP.

In a second experiment our interest was to study the reorientation relaxation processes. In figures 3(a) and 3(b) are reported both τ_{on} and τ_{off} for NP and the M7 mixture, respectively. From the figures it is possible to observe that the characteristic times τ_{off} are, within the errors, constant; i.e. independent of the amplitudes of the applied voltage, as expected. The average values of τ_{off}, denoted by the full straight lines, were 7.8 ± 0.5 s for NP and 10.3 ± 0.5 s for M7.

As regards the τ_{on} times, the switch-on time decreases with the applied voltage, as described by equation (3a). By using the experimental values for E_{th} and τ_{off} in equations (1) and (3b), and fitting the τ_{on} data by means of equation (3a), we obtained the following parameters for the material NP: $\gamma_1^* \approx 17$ cP, $|\Delta\varepsilon| \approx 0.018$ (c.g.s. units) and $K_{33} = 1.82 \times 10^{-7}$ dyne. Following the same calculations for the mixture M7, we obtained: $\gamma_1^* = 147$ cP, $|\Delta\varepsilon| = 0.137$ (c.g.s. units) and $K_{33} = 10.5 \times 10^{-7}$ dyne. In figures 3(a) and 3(b), the full lines connecting the τ_{on} (black circles) switching times represent the best fit made by means of equation (3a).

The values reported in the literature [1] for M7 are the following: the rotational viscosity (determined by the small pulse magnetic field technique) is $\gamma_1 = 41$ cP; the dielectric anisotropy (determined from the complex impedance) is $\Delta\varepsilon = -0.31$ and the bend elastic constant is $K_{33} = 11.6 \times 10^{-7}$ dyne. To our knowledge, there are no data in the literature regarding the material NP.

3. Electrohydrodynamic instabilities under a.c. electric fields

Convective instabilities under electric fields in liquid crystals have already been the subject of several studies, both theoretical and experimental. Let us briefly summarize the main features of the Carr–Helfrich mechanism [6, 7] to explain the occurrence of EHD instabilities for an applied d.c. electric field, in the case of materials

with negative dielectric anisotropy $\Delta\varepsilon = \varepsilon_{\parallel} - \varepsilon_{\perp} < 0$ and positive conductive anisotropy $\Delta\sigma = \sigma_{\parallel} - \sigma_{\perp} > 0$, where $\sigma_{\parallel}$ and $\sigma_{\perp}$ are the electrical conductivities parallel and perpendicular to the optical axis, respectively.

Let us consider a homogeneous planar uniaxial texture where, with respect to the case of figure 1, the molecules now lie parallel to the glass surfaces. A bend distortion, due to thermal fluctuations in the director field gives rise, because of the conductive anisotropy and under the action of the external electric field applied perpendicularly to the glass plates, to a space charge in the director field. In these regions the medium moves with opposite velocity under the action of the electric forces. Because of this velocity gradient, a destabilizing viscous torque will appear, while the electric torque due to the external applied field has a stabilizing effect. The charge separation leads to a transverse component of the electric field, which in turn produces a destabilizing dielectric torque. When the applied electric field reaches a critical value that makes the total torque destabilizing, the instabilities will appear [8, 9]. These are the well known Williams–Kasputin domains, with a spatial periodicity comparable to the sample thickness. The threshold voltage is independent of sample thickness.

In the case of sinusoidal excitation, the Carr–Helfrich mechanism keeps its validity, leading to a characteristic time: the relation time τ of the space charges along the direction of the director [10] (conducting regime).

In the conducting regime, produced at frequencies ω of the external applied electric field lower than τ^{-1}, the volume electric charge oscillates almost in phase with the electric field. The threshold voltage in the conducting regime is [3]:

$$V_{\text{th}} = \mathbf{E}_{\text{th}}\, d = V_{\text{th}}(0)\left[\frac{1 + \omega^2 \tau^2}{\xi^2 - (1 + \omega^2 \tau^2)}\right] \quad (5)$$

where

$$\xi^2 = \left(1 - \frac{\sigma_{\perp}\varepsilon_{\parallel}}{\sigma_{\parallel}\varepsilon_{\perp}}\right)\left(1 + \frac{\alpha_2\,\varepsilon_{\parallel}}{\eta_1\,\Delta\varepsilon}\right)$$

η_1 being the coefficient of viscosity defined according to Gahwiller [11].

Moreover, when the frequency of the applied electric field exceeds a certain value $\omega_c \gg \tau^{-1}$ the onset of instability is manifested optically by parallel striations (dielectric regime). In the dielectric regime the space charge oscillates weakly about a certain mean value. The threshold voltage is proportional to the sample thickness and the threshold electric field varies as $\omega^{1/2}$ [3]:

$$\mathbf{E}_{\text{th}}^2 = \frac{4\eta_{\text{eff}}\,\omega}{2\pi\left[1 - \left(\dfrac{1}{\xi^2}\right)\right]\sigma_{\text{eff}}\,\tau} \quad (6)$$

where η_{eff} and σ_{eff} are, respectively, the effective viscosity and conductivity of the material [3].

The inclusion of an inertial term connected with the change of velocity with time in the equations of nemato-dynamics leads to the prediction of a further high frequency mode involving steady-state motion of the liquid crystal and a stationary distribution of the director (high frequency inertia anisotropic mode) [12]. The threshold voltage varies as:

$$V_{\text{th}} = \mathbf{E}_{\text{th}}\, d \approx \omega \left[\frac{\pi \bar{\varepsilon} \bar{K}}{\bar{\sigma}(\sigma_\parallel - \sigma_\perp)} \right]^{1/2} \qquad (7)$$

where $\bar{\varepsilon}$, $\bar{K}$ and $\bar{\sigma}$ are average values of the dielectric, elastic and conductivity constants, respectively [12].

The domains of the high frequency inertia anisotropic mode have a size greater than the cell thickness and are oriented perpendicularly to the initial orientation of the director. Moreover, the conducting regime and the high frequency inertia anisotropic mode correspond to steady-state motion of the liquid crystal (in the plane of the liquid crystal layer in the case of the high frequency mode [12, 13]) and stationary deviation of the director. On the other hand, in the dielectric regime the oscillations of the director and the velocity of the liquid crystal are in phase with the external applied field.

3.1. *Experiments and results*

Now we report the observations made by means of electro-optical techniques of electrohydrodynamic instabilities in the non-polar materials $0d_3\text{CCO2}$ and in its mixture with MBBA. To test our materials we used electro-optic sandwich-like cells. Planar orientation was achieved by coating the clean glass plates with ACM-72, a polymeric surface aligning material (Atomergic Chemetals Corp.) which ensures planar alignment with a small (less than 2°) pretilt. A 0.05 wt % solution of ACM-72 in deionized water was prepared; the glass plates were immersed in this for 3 min and then removed with a slow vertical motion. The plates were then dried in an oven at 120°C for 20 min and finally buffed about 20 times unidirectionally with a lens cleaning tissue (Whatman).

Observations of electrohydrodynamic structures were made by polarizing optical microscopy using an Axioskop Pol equipped with a Linkam CO 600 heating stage. Video microscopy was performed using a 3CCD colour camera TCM 112 (by GDS Electronic). The samples were kept at a constant temperature of 25°C. The wave-form generator driving the bipolar operational power supply/amplifier generated the sinusoidal signal. The external electric field was applied perpendicularly to the glass plates. Figure 4 shows the behaviour of the threshold field $\mathbf{E}$ of the EHD instabilities as a function of angular
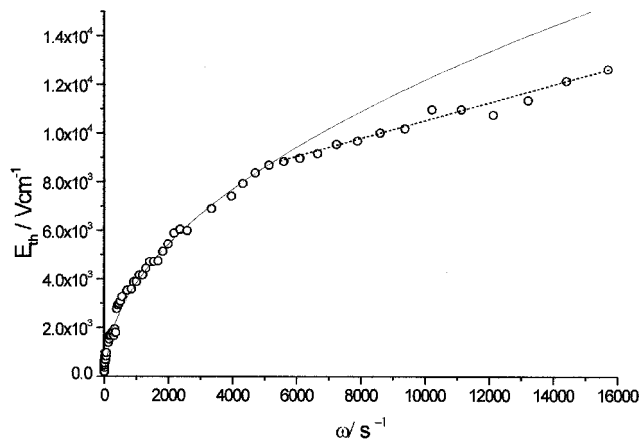

Figure 4. The behaviour of the threshold field of the EHD instabilities as a function of angular frequency of the sinusoidal signal applied to the planar aligned cell 36 μm thick, relative to the non-polar compound (NP). The full line represents the best fit made by means of equation (6). The line representing the fit has been extended at higher frequencies to highlight the subsequent regime. The dotted line represents a fit made by using a linear function.

frequency of the sinusoidal signal applied to the planar aligned 36 μm thick cell, relative to the non-polar compound. From the analysis of the figure it is possible to identify two different regimes: at low frequencies (less than $6000\,\text{s}^{-1}$), there is first a purely dielectric regime $\mathbf{E} \sim \omega^{1/2}$. For higher frequencies we find a linear regime $\mathbf{E} \sim \omega$ (high frequency inertia anisotropic mode [12]).

It is worthwhile noting that, for this material (NP), the conductive regime is absent. By fitting the experimental data of the dielectric regime in figure 4 by means of equation (6) (full line in the figure), we obtained the values of some physical parameters for NP. In particular, this gives the effective viscosity $\eta_{\text{eff}} = 1.02\,\text{cP}$, the effective conductivity $\sigma_{\text{eff}} = 16.2 \times 10^{-11}\,\Omega^{-1}\,\text{cm}^{-1}$, while the anisotropic parameter and the dielectric relaxation time are $\xi^2 = 2.17$ and $\tau = 5 \times 10^{-5}\,\text{s}$, respectively. The dotted line in figure 4 represents a fit made by a linear function.

Figure 5 concerns the behaviour of the threshold field for the mixture of 90 wt % of the non-polar liquid crystal NP with 10 wt % of MBBA. Also in this case, we observed a pure dielectric regime at lower frequencies followed by a regime depending linearly on the frequency of the applied electric field. By fitting the data of the dielectric regime of figure 5 (full line), we obtained an effective viscosity $\eta_{\text{eff}} = 5.9\,\text{cP}$ and an electric conductivity $\sigma_{\text{eff}} = 3.1 \times 10^{-10}\,\Omega^{-1}\,\text{cm}^{-1}$. The dotted line in figure 5 represents a fit made by a linear function.

The mixture of 50 wt % of non-polar material NP and 50 wt % of the nematic liquid crystal MBBA exhibits a well defined conducting regime followed, at higher frequencies, by a dielectric regime (see figure 6). At the highest frequencies it is possible to identify a linear
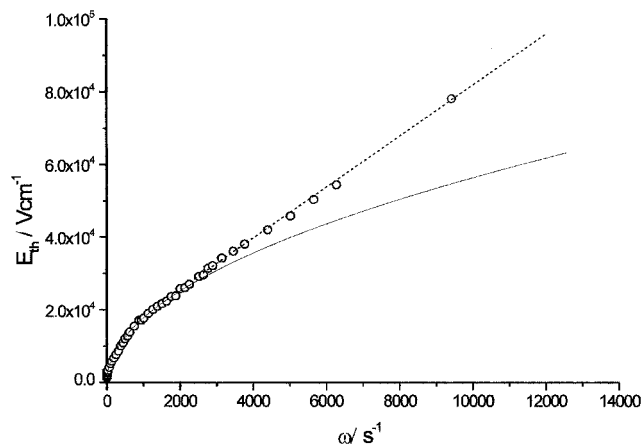
Figure 5.   The behaviour of the threshold field for the mixture of 90 wt % of non-polar liquid crystal NP with 10 wt % of MBBA. The full line represents the best fit made by means of equation (6). The line representing the fit has been extended at higher frequencies to highlight the subsequent regime. The dotted line represents a fit made by using a linear function.
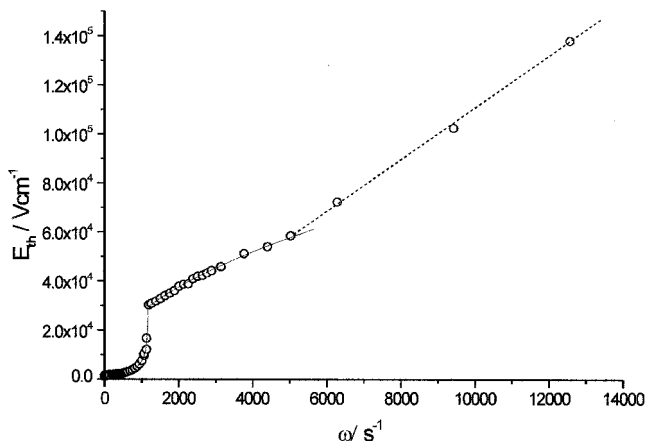

Figure 6.   The threshold field of the EHD instabilities as a function of angular frequency of the sinusoidal signal applied to the planar aligned cell 36 µm thick, relative to the mixture of 50 wt % of the non-polar material NP and 50 wt % of the nematic liquid crystal MBBA. It is possible to observe three different regimes. The full lines represent the best fits made by means of equations (5) and (6). The dotted line represents a fit made by using a linear function.

behaviour of the threshold that suggests the presence again of a high frequency inertia anisotropic mode in this case. By fitting the data of figure 6 we obtained a cut-off frequency $\omega_c = 1286 \, s^{-1}$, a value of the effective viscosity $\eta_{eff} = 6.8 \, cP$, and an effective conductivity $\sigma_{eff} = 3.1 \times 10^{-10} \, \Omega^{-1} \, cm^{-1}$. Also in this figure the dotted line represents a fit made by a linear function. It is evident that the presence of MBBA in a small quantity (10 wt %) does not change significantly the dielectric behaviour of $0d_3CCO2$, while increasing the percentage (50 wt %) does affect the response.

It is interesting to note that the slopes of the curves fitting the linear regimes are different for the materials analysed. Actually, the slope depends on the physical parameters of the materials that are obviously different for the non-polar compound and its mixture see equation (7).

4.   Conclusions

The non-polar liquid crystal $0d_3CCO2$ (acronym NP) is a new material that exhibits both low viscosity and low optical anisotropy. These properties are of great interest in liquid crystals, because they lead to short response times and the materials can therefore find several applications in liquid crystal displays. Our goal was to characterize the electro-optical properties of this new material and its mixtures with MBBA. Moreover, we wished to verify the role of the molecular dipole in the establishment of electro-convective instabilities (Williams–Kasputin domains). From our experiments, it is clear that the absence of a molecular dipole (or the presence of small dipole such as in the case of the mixture of 90 wt % of the non-polar compound NP and 10 wt % of MBBA) inhibits the establishment of Williams–Kasputin domains, so that the dielectric regime spreads to low frequencies of the externally applied electric field. Moreover, at the highest frequencies of the externally applied electric field, we always observed a high frequency inertia anisotropic mode, (including the case of the mixture of 50 wt % of the non-polar compound with MBBA).

References

[1] SCHADT, M., BUCHECKER, R., and MULLER, K., 1989, *Liq. Cryst.*, **5,** 293.
[2] DE GENNES, P. G., and PROST, J., 1993, *The Physics of Liquid Crystals*, 2nd Edn (Oxford: Oxford University Press).
[3] BLINOV, L. M., and CHIGRINOV, V. G., 1994, *Electrooptic Effects in Liquid Crystal Materials* (New York: Springer Verlag).
[4] RAPINI, A., LEGER, L., and MARTINET, A., 1975, *J. Phys. Fr.*, **C1-36,** 189.
[5] LESLIE, F. M., 1979, *Advances in Liquid Crystals*, Vol. 4, edited by G. H. Brown (New York: Academic Press), pp. 1–75.
[6] CARR, E. F., 1963, *J. chem. Phys.*, **39,** 1979.
[7] HELFRICH, W., 1969, *J. chem. Phys.*, **51,** 4092.
[8] SMITH, I. W., GALERNE, Y., LAGERWALL, S. T., DUBOIS-VIOLETTE, E., and DURAND, G., 1975, *J. Phys. Fr.*, **C1-36,** 237.
[9] SCARAMUZZA, N., PAGNOTTA, M. C., and PUCCI, D., 1994, *Mol. Cryst. liq. Cryst.*, **239,** 195.
[10] DUBOIS-VIOLETTE, E., DE GENNES, P. G., and PARODI, O., 1971, *J. Phys. Fr.*, **32,** 305.
[11] GAHWILLER, C., 1971, *Phys. Lett.*, **36A,** 311.
[12] PIKIN, S. A., and CHIGRINOV, V. G., 1980, *Soviet Physics: JETP*, **51,** 123.
[13] TRUFANOV, A. N., BLINOV, L. M., and BARNIK, M. I., 1980, *Soviet Physics: JETP*, **51,** 314.